

A Fast Frequency Sweep – Green’s Function Based Analysis of Substrate Integrated Waveguide

Elnaz ABAEI¹, Giandomenico AMENDOLA², Emilio ARNIERI²,
Sandra COSTANZO², Esfandiar MEHRSHAHI¹

¹ Dept. of Electrical Engineering Shahid Beheshti University, G. C. Tehran, IRAN,

² Dept. of Electronics, Computer and System Sciences (DEIS) University of Calabria – 87036 Rende (CS) ITALY

el_abaei3086@yahoo.com, amendola@deis.unical.it, earnieri@deis.unical.it, costanzo@deis.unical.it, mehr@sbu.ac.ir

Abstract. *In this paper, a fast frequency sweep technique is applied to the analysis of Substrate Integrated Waveguides performed with a Green’s function technique. The well-known Asymptotic Waveform Evaluation technique is used to extract the Padè approximation of the frequency response of Substrate Integrated Waveguides. The analysis is extended to a large frequency range by adopting the Complex Frequency Hopping algorithm. It is shown that, with this technique, CPU time can be reduced by almost one order of magnitude with respect to a point by point computation.*

Keywords

Green’s function methods, Substrate integrated waveguide, SIW, Asymptotic Waveform Evaluation, AWE, Complex Frequency Hopping, CFH.

1. Introduction

Since their introduction [1], Substrate Integrated Waveguides (SIW) have been used to realize several microwave devices [2]-[7]. SIWs may be implemented in both LTCC and more conventional and cheaper PCB technology, thus offering a low cost alternative to metallic waveguides and printed lines. For this reason, in the last years the number of research papers devoted to the design of SIW based devices has increased steadily. Filters, power dividers/combiners, antennas and active devices have been studied and successfully realized [2], [8], [9]. The availability of powerful commercial software packages, mainly based on FEM or FDTD techniques, makes the analysis of SIW structures smooth. However, more effective approaches with reduced computational time have been proposed. In [10], the Boundary Integral Resonant Mode Expansion (BI-RME) was used, while in [11] a single mode analysis was proposed. In [12], [13], [14] the authors present an analysis method adopting the dyadic Green’s function of an infinite parallel plate structures. All these techniques, even if more efficient than general purpose software packages, can be further accelerated adopting fast interpolation methods which rely on model order reduction

techniques. Among them the Asymptotic Waveform Evaluation (AWE) moment matching technique [15], [16] coupled to a Padè rational expansion [17] is the most known technique which has been already proposed to speed up the solution of electromagnetic problems. A first application of AWE to the analysis of SIW structures is discussed in [18], where a fast frequency sweep is adopted to accelerate the solution of a hybrid modal technique.

In this paper, the AWE – Padè method is used to improve the performance of the Green’s function based analysis originally presented in [12]. High accuracy and significant computation time reduction up to 80-90% are obtained by adopting interpolation polynomials of order 2, while typical order ranging from 2 up to 36 are required by similar interpolation procedures, such as the Cauchy’s method [19].

The paper is organized as follows. In Section II, a brief account of the theory related to the Green’s function method is presented. In Section III, a detailed explanation of the implemented AWE – Padè technique is provided, while numerical validations on three different cases of passive SIW devices are discussed in Section IV. Conclusions are finally outlined in Section V.

2. Green’s Function Analysis of SIWs

SIW structures are modeled in [12] as an ensemble of via holes embedded into a parallel plate waveguide, and their analysis is efficiently performed by using the dyadic Green’s functions of the parallel plate, and considering the scattering by metallic vias. Only magnetic current sources are taken into account. Under these conditions, the total magnetic field into the SIW structures can be expressed as the sum of two contributions, namely:

$$\mathbf{H}(\mathbf{r}) = -j\omega\epsilon\int d\mathbf{p}'\overline{\mathbf{G}}_{PPW}(\mathbf{r},\mathbf{r}')\cdot\mathbf{J}_M(\mathbf{r}') + \mathbf{H}_{SCyl}(\mathbf{r}) \quad (1)$$

where the integral represents the parallel plate contribution, and the second term gives the contribution due to the field scattered by vias.

In the previous expression, $\mathbf{J}_M(\mathbf{r})$ is the magnetic current representing the source, while $\overline{\mathbf{G}}_{PPW}(\mathbf{r},\mathbf{r}')$ is the

magnetic dyadic Green's function, which can be conveniently expressed in terms of cylindrical wave functions as follows [12]:

$$\begin{aligned} \bar{\mathbf{G}}_{ppw}(\mathbf{r}, \mathbf{r}') &= \left(\frac{-1}{k}\right) \hat{\mathbf{z}} \hat{\mathbf{z}}' \delta(\mathbf{r} - \mathbf{r}') \\ &\quad - j \sum_m \left(1 - \frac{\delta_{m0}}{2}\right) \frac{1}{k_{\rho m}^2 h} \\ &\quad [(\nabla \times \hat{\mathbf{z}})(\nabla \times \hat{\mathbf{z}}')] H_0^{(2)}(k_{\rho m} |\boldsymbol{\rho} - \boldsymbol{\rho}'|) \\ &\quad \cos(k_{zm} z) \cos(k_{zm} z') \\ &\quad + \frac{1}{k^2} (\nabla \times \nabla \times \hat{\mathbf{z}})(\nabla \times \nabla \times \hat{\mathbf{z}}') H_0^{(2)}(k_{\rho m} |\boldsymbol{\rho} - \boldsymbol{\rho}'|) \\ &\quad \sin(k_{zm} z) \sin(k_{zm} z') \end{aligned} \quad (2)$$

In the previous equation, $k = \omega \sqrt{\mu \epsilon_0 \epsilon_r}$, $k_{zm} = \frac{m\pi}{d}$, d being the parallel plate height, and $k_{\rho m} = \sqrt{k^2 - k_{zm}^2}$. The field scattered by the vias is expressed in terms of a series of vector cylindrical wavefunctions as:

$$\mathbf{H}_{SCyl}(\mathbf{r}) = \sum_{l,n,m} [\mathbf{M}_n(k_{\rho m}, k_{zm}, \boldsymbol{\rho} - \boldsymbol{\rho}_l, h - z) A_{n,m,l}^M + \mathbf{N}_n(k_{\rho m}, k_{zm}, \boldsymbol{\rho} - \boldsymbol{\rho}_l, h - z) A_{n,m,l}^N] \quad (3)$$

where

$$\begin{aligned} \mathbf{M}_n(k_{\rho m}, k_{zm}, \boldsymbol{\rho}, z) &= \\ \nabla \times J_n(k_{\rho m} \rho) e^{-jn\phi} \cos(k_{zm} z) \hat{\mathbf{z}} \quad \rho \leq \rho' \\ \nabla \times H_n^{(2)}(k_{\rho m} \rho) e^{-jn\phi} \cos(k_{zm} z) \hat{\mathbf{z}} \quad \rho > \rho' \\ \mathbf{N}_n(k_{\rho m}, k_{zm}, \boldsymbol{\rho}, z) &= \\ \frac{1}{k} \nabla \times \nabla \times J_n(k_{\rho m} \rho) e^{-jn\phi} \sin(k_{zm} z) \hat{\mathbf{z}} \quad \rho \leq \rho' \\ \frac{1}{k} \nabla \times \nabla \times H_n^{(2)}(k_{\rho m} \rho) e^{-jn\phi} \sin(k_{zm} z) \hat{\mathbf{z}} \quad \rho > \rho' \end{aligned} \quad (4)$$

Coefficients into (3) are determined by solving the following matrix equations for the TE and TM modes:

$$\Gamma_{q,r,m}^{TM,TE} = \sum_{l \neq q} \sum_n L_{q,r,m,l,m}^{TM,TE} A_{m,n,l}^{M,N} + A_{m,r,q}^{M,N} \quad (5)$$

where

$$L_{q,r,m,l,n}^{TM} = \frac{J_r(k_{\rho m} a_q)}{H_r^{(2)}(k_{\rho m} a_q)} H_{n-r}^{(2)}(k_{\rho m} \rho_{lq}) e^{-j(n-r)\phi_{lq}}, \quad (6)$$

$$\Gamma_{q,r,m}^{TM} = \frac{-J_r(k_{\rho m})}{H_r^{(2)}(k_{\rho m} a_q)} v_{m,r,q}^{TM}, \quad (7)$$

$$v_{m,r,q}^{TM} = -j\omega \epsilon \frac{j(-1)^{r-m} \left(1 - \frac{\delta_{m0}}{2}\right)}{2k_{\rho m}^2 h} \quad (8)$$

$$\int d\mathbf{r}' \mathbf{M}_{-n}'(k_{\rho m}, k_{zm}, \boldsymbol{\rho} - \boldsymbol{\rho}', z') \cdot \mathbf{J}_M(\mathbf{r}'),$$

$$L_{q,r,m,l,n}^{TE} = \frac{J_r'(k_{\rho m})}{H_r^{(2)'}(k_{\rho m} a_q)} H_{n-r}^{(2)}(k_{\rho m} \rho_{lq}) e^{-j(n-r)\phi_{lq}} \quad (9)$$

$$\Gamma_{q,r,m}^{TE} = \frac{-J_r'(k_{\rho m})}{H_r^{(2)'}(k_{\rho m} a_q)} v_{m,r,q}^{TE}, \quad (10)$$

$$v_{m,r,q}^{TE} = -j\omega \epsilon \frac{j(-1)^{r-m} \left(1 - \frac{\delta_{m0}}{2}\right)}{2k_{\rho m}^2 h} \quad (11)$$

$$\int d\mathbf{r}' \mathbf{N}_{-n}'(k_{\rho m}, k_{zm}, \boldsymbol{\rho} - \boldsymbol{\rho}', z') \cdot \mathbf{J}_M(\mathbf{r}')$$

In the previous equations, the terms $v_{m,r,q}^{TM}$, $v_{m,r,q}^{TE}$ are the excitation coefficients relevant to the current source $\mathbf{J}_M(\mathbf{r})$. Once the coefficients in (5) and the excitation coefficients are known, the admittances at the ports are calculated as:

$$Y^{(p_i, p_j)} = \frac{-\int_{S_{p_j}} d\mathbf{r} \mathbf{H}^{p_i}(\mathbf{r}) \cdot \mathbf{J}_M^{p_j}(\mathbf{r})}{|V|^2} \quad (12)$$

where $\mathbf{H}^{p_i}(\mathbf{r})$ is the total magnetic field due to the current $\mathbf{J}_M^{p_i}$ on port p_i , S_{p_j} is the surface of port p_j and $\mathbf{J}_M^{p_j}$ is the current impressed on port p_j . More details on formula (12) and how it specializes to coaxial and waveguide ports are given in [12].

3. Fast Frequency Sweep

As remarked in the introduction, the most used and straightforward method to achieve a fast frequency sweep is the AWE technique [15], [16]. The method applies to any transfer functions or, more in general, to any system matrix, in the frequency domain as well as in the s-domain, to synthesize a reduced order model giving a good approximation of the frequency response of the original system.

Given a matrix equation of the form:

$$\bar{\mathbf{A}}(\omega) \mathbf{x}(\omega) = \mathbf{b}(\omega), \quad (13)$$

the solution of the system is expanded around ω_0 in a Taylor series as :

$$\mathbf{x}(\omega) = \sum_{n=0}^{\infty} \mathbf{M}_n (\omega - \omega_0)^n \quad (14)$$

where \mathbf{M}_n are the moments that can be recursively calculated as:

$$\mathbf{M}_n = \bar{\mathbf{A}}(\omega_0)^{-1} \left[\frac{\mathbf{b}^{(n)}(\omega_0)}{n!} - \sum_{r=0}^{n-1} \left(\frac{(1-\delta_{r0}) \bar{\mathbf{A}}^{(r)}(\omega_0) \mathbf{M}_{(n-r)}}{r!} \right) \right] \quad (15)$$

Taylor expansion (14) can be used to find a rational Padé' expansion [17] of $\mathbf{x}(\omega)$ which is valid over a wider frequency range.

The AWE technique may be used to find the Padé approximation of the frequency response of the device under analysis by directly operating on the output parameters, such as S matrix. Even if being the most rapid way to apply the method, this approach does not produce significant performance improvements. To further reduce

the computation time, the AWE technique is applied in this paper to find a moment expansion (14) for the coefficients $A_{n,m,l}^{M,N}$ into expansion (5). As a matter of fact, fill time and inversion of (6) are the most time consuming tasks to be performed. Once the moments expansion of coefficients into (5) is known, it can be used to efficiently compute the Padè approximation of the port admittances (12) and then of the S parameters relative to the device under analysis. Notice that, as the elements of Γ and L are expressed into analytical form, moments (15) may be computed in a closed form because they mainly contain derivatives of Hankel and Bessel functions. The main difficulty remains in the lengthy and tedious algebra, because the derivatives of Hankel and Bessel functions are easily and efficiently derived recursively with a minimum computational effort. In the appendix are reported, as illustrative example, the derivatives of expression (6) for the TM case up to the fourth order. Derivatives of other terms are determined in a similar manner.

As it is well known, AWE method becomes quickly ill conditioned when the number of moments increases, therefore increasing the number of moments used in the approximation does not guarantee a better fit. One can say that the method remains applicable if the number of moments required stays below 8 [21]. This limitation restricts the range of validity of the Padè' rational expansion on a single frequency point. To overcome this problem, the Complex Frequency Hopping (CFH) technique has been introduced in [20]. Once the frequency range of interest (f_{min} , f_{max}) is fixed, the algorithm straightforwardly selects a minimum number of points with respect to which the expansion of coefficients into expression (5) is performed according to Padè; the number of points (hops) required to obtain an accurate result over the specified frequency range is controlled by a binary search algorithm [20]. The steps involved in the search algorithm are summarized below:

1. Set $f_L = f_{min}$ and $f_H = f_{max}$;
2. Evaluate the Padè' expansion of the port admittance around f_L ($Y_L(f)$) using the AWE moment expansion of the coefficient into (5);
3. Evaluate the Padè' expansion of the port admittance around f_H : ($Y_H(f)$) using the AWE moment expansion of the coefficient into (5);
4. Set $f_{mid} = (f_L + f_H) / 2$ and evaluate $Y_L(f_{mid})$ and $Y_H(f_{mid})$;
5. IF $(| Y_L(f_{mid}) - Y_H(f_{mid}) | / Y_H(f_{mid})) < \epsilon$ then Stop. ELSE evaluate the Padè' expansion of the port admittance around f_{mid} ($Y_{mid}(f)$); repeat steps 2-5 in the range $f_L..f_{mid}$ and $f_{mid}..f_H$.

The term ϵ adopted in the algorithm is a predefined percentage error limit.

The Padè approximation of the port admittance $Y(f)$ around a fixed frequency f_0 is evaluated by using two poles and two zeros: comparison with discrete results have shown that this is the best choice for both accuracy and

simulation time. The rational function used in the Padè approximation is defined by its 5 coefficients. $Y(f_0)$ and its derivatives till order four are used to evaluate the 5 unknown coefficients [20]. Derivatives are evaluated by using the forward-difference method, then Padè approximation at each expansion point is obtained with 5 sample frequencies.

4. Numerical Results

The theory presented in the previous paragraphs is implemented into a MATLAB code. Three structures presented in [12] are analyzed in order to test the efficiency and the accuracy of the proposed approach.

4.1 Three-Pole Posts Filter

As a first test, the three pole posts filter presented in [12] is considered. Fig. 1 shows the comparison between the results provided by the CFH technique and that obtained by applying the Green's function method in [12] with a discrete frequency sweep. For comparison, moments of scattering coefficients in (5) are computed using both analytical and numerical derivatives.

A complete agreement between the discrete sweep and the fast sweep responses can be observed, both with numerical and analytical derivatives computation. A percentage error limit of $\epsilon = 0.1$ is used in the CFH for both cases. The calculation of the analytical derivatives improves the method efficiency by reducing the total computation time. As a matter of fact, for a fixed error limit of $\epsilon=0.1$, the adopted procedure provides, when compared to the discrete method, a computation time reduction equal to 78.2 % for the numerical case and equal to 84.3 % for the case of analytical derivatives (see Tab. 1). Comparison between numerical and analytical derivatives shows a maximum error of 0.4 %.

Fig. 2 compares results for three error-limit (ϵ) values.

Method	Nr. of expans. points	Mean Absolute Error (MAE) of S12	Total Time (112 frequency points)	Time reduction
Discrete simulation [12]	112	0	130.6 sec	-
Numerical CFH ($\epsilon = 0.1$)	5	0.0066	28.5 sec	78,2%
Analytical CFH ($\epsilon = 0.1$)	5	0.0087	20.5 sec	84,3%
Analytical CFH ($\epsilon = 0.2$)	4	0.0167	16.7 sec	87,2%
Analytical CFH ($\epsilon = 0.6$)	3	0.0479	12.2 sec	90,7%

Tab. 1. CPU Simulation time for the post filter. Results obtained on an AMD Athlon(tm) II*2 250 processor 3.00 GHz 4.00 GB RAM.

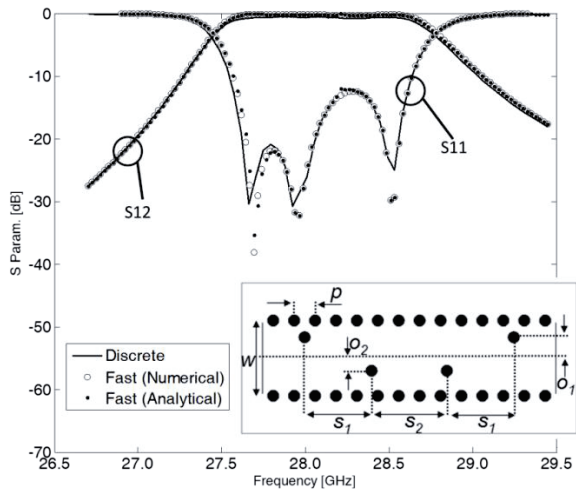


Fig. 1. Frequency domain analysis of the three pole posts filter proposed in [12] compared to the CFH analysis. (Numerical and Analytical calculated derivatives). $p = 1.525$ mm, $W = 5.563$ mm, $S_1 = 4.71$ mm, $S_2 = 5.11$ mm, $O_1 = 1.01$ mm, $O_2 = 0$ mm, Relative dielectric constant = 2.2, $h = 0.787$ mm.

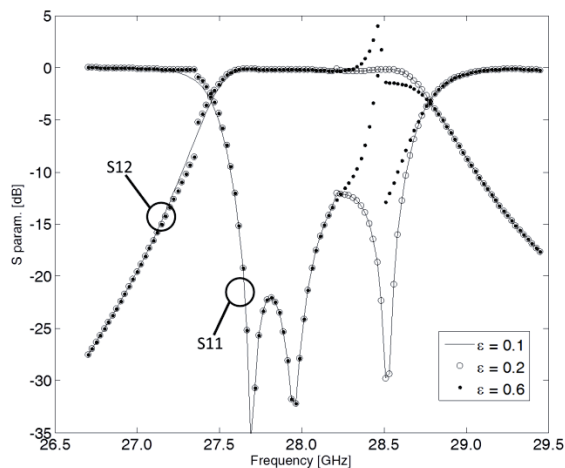


Fig. 2. Results comparison for three error-limit (ϵ) values.

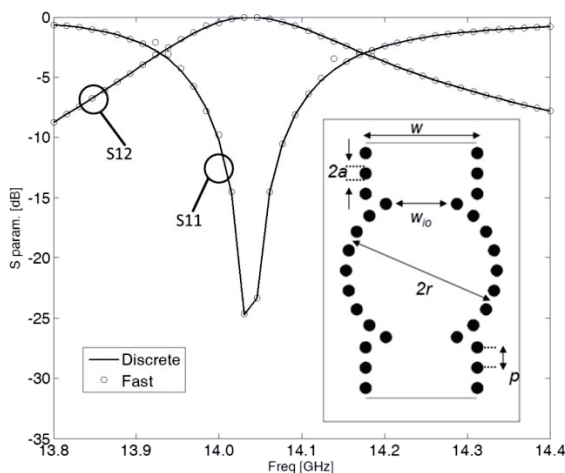


Fig. 3. Circular filter. Error-limit $\epsilon = 0.2$ $W = 3.8$ mm, $W_{io} = 1.683$ mm, $a = 0.2$ mm, $r = 2.4$ mm, $p = 0.7$ mm, Relative dielectric constant = 9.9, $h = 0.380$ mm.

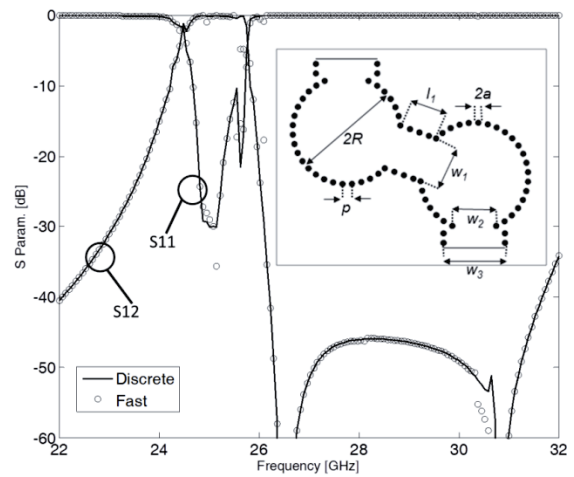


Fig. 4. Dual coupled cavity filter. Error-limit $\epsilon = 0.3$. $W_1 = 4.08$ mm, $W_2 = 3.93$ mm, $W_3 = 5.50$ mm, $a = 0.2$ mm, $p = 0.851$ mm, $l_1 = 3.404$ mm, $R = 4.83$ mm, $a = 2.55$ mm. Relative dielectric constant = 2.2, $h = 0.5$ mm.

As expected, by reducing the error tolerance, more accurate results are obtained; on the other hand, lower values of ϵ require a larger number of expansion points. Tab. 1 also shows the comparison between CPU time obtained by applying the proposed CFH method and a discrete simulation. A good agreement with this latter method [12] is obtained by enforcing an error-limit (ϵ) of 0.2. In this case, a computation time reduction of 87.2 % is derived.

4.2 Circular Filter

Fig. 3 shows the scattering parameters of a simple circular cavity filter presented in [12]. A good agreement with discrete simulations [12] is obtained by enforcing an error-limit (ϵ) of 0.2. In this case, a speed up of 90 % is achieved.

4.3 Dual Coupled Cavity Filter

Finally, a more complex dual-coupled cavity filter based on circular resonators [12] is considered as validation example. Fig. 4 shows and compares the fast results with the discrete ones. The agreement between the simulations is very good. An error-limit (ϵ) of 0.3 is enforced; in this case, a computation times reduction of 79 % is achieved.

5. Conclusions

In this paper, the AWE – Padè method has been used in conjunction with the CFH technique to improve the performance of the Green’s function based analysis presented in [12]. The AWE technique has been applied to find a moment expansion of the scattering coefficients used in [12], subsequently adopted to efficiently compute the Padè approximation of the port admittances and the S parameters of the device under analysis.

The method has been applied to known cases taken from literature. Very accurate results, with a computation time reduction up to 80-90 %, have been obtained. The proposed technique can be efficiently applied to the analysis and design of SIW devices.

Appendix

In this appendix, the derivatives of equation (6) are presented. Derivatives of the other components can be derived in a similar manner.

Let us consider the expression:

$$L_{q,r,m,l,n} = \left[\frac{J_r(k_{\rho m} a_q)}{H_r^{(2)}(k_{\rho m} a_q)} \right] H_{n-r}^{(2)}(k_{\rho m} \rho_{lq}) e^{-j(n-r)\phi_{lq}}. \quad (A1)$$

It is considered as the product of three terms. Derivatives with respect to $k_{\rho m}$ can be considered first. Derivatives with respect to ω can be later computed with the use of the chain rule. Indicating the first term as:

$$\chi(k_{\rho m}) = \left[\frac{J_r(k_{\rho m} a_q)}{H_r^{(2)}(k_{\rho m} a_q)} \right] \quad (A2)$$

we obtain:

$$\frac{\partial \chi}{\partial k_{\rho m}} = a_q \frac{2j}{\pi k_{\rho m} a_q} \frac{1}{[H_r^{(2)}(k_{\rho m} a_q)]^2}, \quad (A3)$$

$$\frac{\partial^2 \chi}{\partial k_{\rho m}^2} = -a_q^2 \frac{2j}{\pi} \Phi(k_{\rho m}), \quad (A4)$$

$$\frac{\partial^3 \chi}{\partial k_{\rho m}^3} = -a_q^3 \frac{2j}{\pi} \frac{2}{k_{\rho m} a_q} \{ \Phi(k_{\rho m}) + \Psi(k_{\rho m}) \}, \quad (A5)$$

$$\frac{\partial^4 \chi}{\partial k_{\rho m}^4} = a_q^4 \frac{2j}{\pi} \left\{ \frac{6}{(k_{\rho m} a_q)^2} (\Phi(k_{\rho m}) + \Psi(k_{\rho m})) - \frac{2}{(k_{\rho m} a_q)} \Psi'(k_{\rho m}) \right\} \quad (A6)$$

where:

$$\Phi(k_{\rho m}) = \frac{-1}{(k_{\rho m} a_q)^2} \frac{1}{[H_r^{(2)}(k_{\rho m} a_q)]^2} + \frac{-1}{k_{\rho m} a_q} \frac{2[H_r^{(2)}(k_{\rho m} a_q)]'}{[H_r^{(2)}(k_{\rho m} a_q)]^3}, \quad (A7)$$

$$\Psi(k_{\rho m}) = \frac{[H_r^{(2)}(k_{\rho m} a_q)]'' H_r^{(2)}(k_{\rho m} a_q) - 3[H_r^{(2)}(k_{\rho m} a_q)]'^2}{H_r^{(2)}(k_{\rho m} a_q)^4}, \quad (A8)$$

$$\begin{aligned} \Psi'(k_{\rho m}) &= \frac{H_r^{(2)}(k_{\rho m} a_q)'' H_r^{(2)}(k_{\rho m} a_q)}{H_r^{(2)}(k_{\rho m} a_q)^4} + \\ &- \frac{5H_r^{(2)}(k_{\rho m} a_q)' H_r^{(2)}(k_{\rho m} a_q)''}{H_r^{(2)}(k_{\rho m} a_q)^4} \\ &- 4\Psi(k_{\rho m}) \frac{H_r^{(2)}(k_{\rho m} a_q)'}{H_r^{(2)}(k_{\rho m} a_q)} \end{aligned} \quad (A9)$$

The derivatives of function (1) are then computed using the standard formulas relative to the derivative of the product of functions. Notice that, up to know, derivatives with respect to $k_{\rho m}$ have been considered, and AWE has been applied to the coefficients into (5) as functions of the frequency. To do this, derivatives of $k_{\rho m}$ with respect to the frequency are required, which are given below:

$$k_{\rho m} = \sqrt{(\omega \sqrt{\mu_0 \epsilon_0 \epsilon_r})^2 - k_{zm}^2}, \quad (A10)$$

$$\frac{d}{d\omega} k_{\rho m} = \frac{\omega \sqrt{\mu_0 \epsilon_0 \epsilon_r}^2}{k_{\rho m}} \quad (A11)$$

$$\frac{d^2}{d\omega^2} k_{\rho m} = (\sqrt{\mu_0 \epsilon_0 \epsilon_r})^2 \left\{ \frac{1}{k_{\rho m}} - \omega U(\omega) \right\} \quad (A12)$$

where

$$U(\omega) = \frac{k'_{\rho m}}{k_{\rho m}^2}, \quad (A13)$$

$$\frac{d^3}{d\omega^3} k_{\rho m} = -(\sqrt{\mu_0 \epsilon_0 \epsilon_r})^2 \{ 2U(\omega) + \omega U'(\omega) \}, \quad (A14)$$

$$U'(\omega) = \frac{k'''_{\rho m} k_{\rho m} - (k'_{\rho m})^2}{k_{\rho m}^3}, \quad (A15)$$

$$\frac{d^4}{d\omega^4} k_{\rho m} = -(\sqrt{\mu_0 \epsilon_0 \epsilon_r})^2 \{ 3U'(\omega) + \omega U''(\omega) \}, \quad (A16)$$

$$U'' = \frac{k''''_{\rho m} k_{\rho m} - 3k'''_{\rho m} k'_{\rho m}}{k_{\rho m}^3} - 3U'(\omega) \frac{k'_{\rho m}}{k_{\rho m}}. \quad (A17)$$

References

- [1] DESLANDES, D., WU, K. Integrated microstrip and rectangular waveguide in planar form. *IEEE Microwave and Wireless Components Letters*, 2001, vol. 11, no. 2, p. 68 - 70.
- [2] DESLANDES, D., WU, K. Single-substrate integration technique of planar circuits and waveguide filters. *IEEE Transactions on Microwave Theory and Techniques*, 2003, vol. 51, no. 2, p. 593 - 596.
- [3] ZHANG, X.-C., YU, Z.-Y., XU, J. Novel band-pass substrate integrated waveguide (SIW) filter based on complementary split ring resonators (CSRRLs). *Progress In Electromagnetics Research*, 2007, vol. 72, p. 39 - 46.
- [4] ZHONG, C., XU, J., YU, Z., ZHU, Y. Ka-band substrate integrated waveguide Gunn oscillator. *IEEE Microwave and Wireless Components Letters*, 2008, vol. 18, no. 7, p. 461 - 463.
- [5] LIU, C., HUANG, K. A compact substrate integrated waveguide band-pass filter. *Progress in Electromagnetics Research Symposium Proceedings*. Cambridge (USA), 2010, p. 1135 - 1138.
- [6] KIM, K., BYUN, J., LEE, H.-Y. Substrate integrated waveguide Wilkinson power divider with improved isolation performances. *Progress in Electromagnetics Research Letters*, 2010, vol. 19, p. 41 - 48.
- [7] ZHONG, C.-L., XU, J., YU, Z.-Y., WANG, M.-Y., LI, J.-H. Half mode substrate integrated waveguide broadband bandpass filter. *Progress in Electromagnetics Research Letters*, 2008, vol. 4, p. 131 - 138.

- [8] GERMAIN, S., DESLANDES, D., WU, K. Development of substrate integrated waveguide power dividers. In *IEEE 2003. Canadian Conference on Electrical and Computer Engineering, CCECE*. Montreal (Canada), 2003, vol. 3, p. 1921 - 1924.
- [9] PARK, S., OKAJIMA, Y., HIROKAWA, J., ANDO, M. A slotted post-wall waveguide array with interdigital structure for 45° linear and dual polarization. *IEEE Transactions on Antennas and Propagation*, 2005, vol. 53, no. 9, p. 2865 - 2871.
- [10] BOZZI, M., PERREGRINI, L., KE WU Direct determination of multi-mode equivalent circuit models for discontinuities in substrate integrated waveguide technology. In *IEEE MTT-S International Microwave Symposium*. San Francisco (CA, USA), 2006, p. 68 - 71.
- [11] WU, X. H., KISHK, A. A. Hybrid of method of moments and cylindrical eigenfunction expansion to study substrate integrated waveguide circuits. *IEEE Transactions on Microwave Theory and Techniques*, 2008, vol. 56, no. 10, p. 2270 - 2276.
- [12] ARNIERI, E., AMENDOLA, G. Analysis of substrate integrated waveguide structures based on the parallel-plate waveguide Green's function. *IEEE Transactions on Microwave Theory and Techniques*, 2008, vol. 56, no. 7, p.1615 - 1623.
- [13] ARNIERI, E., AMENDOLA, G. Method of moments analysis of slotted substrate integrated waveguide arrays. *IEEE Transactions on Antennas and Propagation*, 2011, vol. 59, no. 4, p. 1148 - 1154.
- [14] ANGIULLI, G., DE CARLO, D., AMENDOLA, G., ARNIERI, E., COSTANZO, E. Support vector regression machines to evaluate resonant frequency of elliptic substrate integrate waveguide resonators. *Progress In Electromagnetics Research*, 2008, vol. 83, p. 107 - 118.
- [15] PILLAGE, L. T., ROHRER, R. A. Asymptotic waveform evaluation for timing analysis. *IEEE Transactions on Computer-Aided Design of Integrated Circuits and Systems*, 1990, vol. 9, no. 4, p. 352 - 366.
- [16] REDDY, C. J., DESHPANDE, M. D. *Application of AWE for RCS Frequency Response Calculations using Method of Moments*. NASA contractor report NASA CR-4758.
- [17] DEY, S., MITTRA, R. Efficient computation of resonant frequencies and quality factors of cavities via a combination of the finite-difference time-domain technique and the Pade approximation. *IEEE Microwave and Guided Wave Letters*, 2008, vol. 8, no. 12, p. 415 - 417.
- [18] BELENGUER, A., ESTEBAN, H., DIAZ, E., BACHILLER, C., CASCON, J., BORJA, V. E. Hybrid technique plus fast frequency sweep for the efficient and accurate analysis of substrate integrated waveguide devices. *IEEE Transactions on Microwave Theory and Techniques*, 2011, vol. 59, no. 3, p. 552 - 560.
- [19] ADVE, R. S., SARKAR, T. K., RAO, S. M., MILLER, E. K., PFLUG, D. R. Application of the Cauchy method for extrapolating/interpolating narrowband system responses. *IEEE Transactions on Microwave Theory and Techniques*, 1997, vol. 45, no. 5, p. 837 - 845.
- [20] CHIPROUT, E., NAKHLA, M. S. Analysis of interconnect networks using complex frequency hopping (CFH). *IEEE Transactions on Computer-Aided Design of Integrated Circuits and Systems*, 1995, vol. 14, no. 2, p. 186 - 200.
- [21] FELDMANN, P., FREUND, R. W. Efficient linear circuit analysis by Pade approximation via the Lanczos process. *IEEE Transactions on Computer-Aided Design of Integrated Circuits and Systems*, 1995, vol. 14, no. 5, p. 639 - 649.